JOURNAL OF OPTOELECTRONICS AND ADVANCED MATERIALS Vol. 15, No. 11 - 12, November ï December 2013, p. 1392 - 1398

Chemical and micro-structural characterization of a copper based shape memory alloy

I. CIMPOESU, S. STANCIU, N. CIMPOESU*, C. MUNTEANU, B. ISTRATE,
A. URSANU DRAGOĶ, D. DANĬ , A. ALEXANDRU, C. NEJNERU
Materials Science Department, Materials Science and Engineering Faculty, Technical University "Gh. Asachi" from Iasi, Str. Prof.dr.doc. D. Mangeron no. 41, Iaşi, 700050, România

A new promising copper based material with shape memory was obtained through classical melting method. The alloy presents shape memory effect in melted state with no thermo-mechanical education applied and with temperature variation it has an interesting behavior. Material microstructure after different heat treatments, like solution annealing with different cooling environments was established with a scanning electrons microscope (SEM) using 2D and 3D features. Different surface characteristics like martensite plates dimensions or orientation was considered for all the material states to establish the influence of the heat treatment conditions on the material microstructure. Complementary atomic force microscope (AFM) was used to realize for a better dimensional characterization. Chemical considerations on the material were made using X-ray diffraction and dispersive energy spectrometry equipments to realize an elemental characterization.

(Received September 3, 2013; accepted November 7, 2013)

Keywords: Shape memory, Cooper, Martensite

1. Introduction

Several Cu-based materials have exhibited the shape-memory effect (SME) and the understanding of their thermal behaviors and microstructure evolutions has brought a significant impact on their applications [1].

With the investigations on martensite transformations shape memory properties have had a strong interest and many kinds of metallic or non-metallic matrices and shape memory materials have been produced. Final products obtained from shape memory materials have been extensively used in the technological area and also in surgery and dentistry [1]. Because of their wide use in the technological world, many kinds of new alloys have been produced for different applications [2].

Shape memory metal alloys based on copper, especially those from CuZnAl system are sensitive materials to heat changes before and after the martensitic transformation and these influences can cause significant changes to the crystallographic characteristics and other transformation parameters.

Comparing to the other shape memory alloys, the copper-based SMAs have been preferred because of their good memory properties and low cost of production [1]. The remarkable properties of SMAa are governed by a reversible structural transformation, type martensitic transformation, between the highly symmetric parent phase (P) and the less ordered martensite (M) solid phases. The martensitic transformation of many copper based shape memory alloys are influenced by quenching and/or post-quench aging. As often claimed, the degree of stabilization depends on the heat treatment conditions. The direct quenching from high temperatures to the martensite phase is the most effective [3]. Martensitic transformations are known as first-order phase transitions associated with a shape change in metals and alloys, and occur by a shear-like mechanism called invariant plain strain [4]. Shape memory effects observed in many alloy systems are a direct result of a thermo-elastic martensitic transformation [5,6]. This transformation is crystallo-graphically reversible and causes the shape recovery mechanism. In order to improve the knowledge about CuZnAl alloys which undergo thermo-elastic martensitic transformation, the X-ray studies are also very important [7].

X-ray analysis can be used to determine the characteristic structural changes that occur after different heat treatments applied or changing the treatment parameters.

The potential application of shape-memory alloys (SMA) in damping devices for civil structures, like buildings and bridges, to smooth out the oscillations produced by earthquakes, winds, etc., has been a subject of increasing interest in recent years. The pseudoelastic effect and the hysteresis cycle associated to the martensitic transformation in SMA are used to dissipate the energy of the oscillations [8, 9]. Few relevant parameters are to be considered in this type of applications. Mainly the hysteresis width associated to the pseudoelastic cycle. The wider the hysteresis is than the larger the dissipated energy will be for every cycle, providing for a more efficient damping device. Secondly, the critical stresses to induce the pseudoelastic effect depend on the working temperature and given by Clapeyron equation [10]. A strong variation of these stresses with temperature will change the stiffness and the resonance frequencies of the civil structures. The performance of damping devices would also be ambient-temperature dependent. In addition, other important parameters to take into account are:

-the evolution of the pseudoelastic cycles during cycling,
-the number of cycles until fracture,
-the evolution of the material itself due to atom diffusion effects, with time and temperatures, etc.

Until now nitinol based alloys have been the most extensively studied materials, using the B2 ź B19ô martensitic transformation as a pseudoelastic mechanism. The average hysteresis width in the first pseudoelastic pullï pull cycle ranges from about 200 MPa to about 400 MPa, depending on several factors, like: specimen preparation method, crystallographic texture, wire diameter or specimen size, working temperature, amount of elongation, deformation velocity, etc. [15]. Niï Ti wires textured along the [1 1 1] 2 direction can undergo about 9% pseudoelastic strain [15].

The pseudoelastic behavior degrades rapidly in the first cycles towards an asymptotic behavior. The final reasonably steady state is reached after a few hundred cycles. The average hysteresis width drops to a value which is roughly (or sometimes less than) one half of its initial value. In addition, non-recoverable strain accumulates in the material during cycling, reducing the length of the pseudoelastic deformation by an amount that could reach up to about 4% of the initial useful length [16], depending on the several afore-mentioned factors. Both effects (the reduction in hysteresis width and the reduction in pseudoelastic strain) will result in a strong reduction in damping capacity during cycling.

Moreover some interesting studies have also been carried out in CuAlBe alloys as applied to damping devices. The ɓ ź 18R transformation in polycrystalline CuAlBe alloys has been chosen for damping prototypes of applications for civil structures, such as family houses [17]. The average hysteresis width in the tensile pseudoelastic behavior of CuAlBe polycrystalline materials ranges from about 20 to 150 MPa, depending on grain size, amount of pseudoelastic deformation, previous thermal treatments, deformation velocity, etc. The pseudoelastic behavior in CuAlBe degrades rapidly in the first cycles towards an asymptotic behavior, similarly to NiTi alloys. The final reasonably steady state is reached after about a hundred cycles. The hysteresis width reduces to a value which is roughly (or sometimes less than) half of its initial value. The pseudoelastic strain in the first cycle can be about 6.5%.

However, this recoverable deformation is reduced by cycling by an amount which depends on the several factors aforementioned [18, 19]. The best value for the relation between transformation stresses and working temperature is dů/dT = 2.2 MPa/K [14], which is much lower than the value for NiTi given above. Very little attention has been paid to the damping capacity in other Cu-based alloys, such as CuAlNi [20,21] or CuAlMn [22], and ferrous alloys such as FeMn-based alloys [23].

In this report, we consider the 18R ź 6R martensite-tomartensite transformation in CuZnAl alloys. These alloys, depending on their composition, can undergo several martensitic transformations between metastable phases, which are induced either by temperature changes or by mechanical stresses [22]. In alloys with electronic concentration e/a = 1.48 and ɓ ź 18R martensitic transformation temperature Ms close to 273 K, when a single crystal is strained in tension at temperatures above Ms, two martensitic transformations can be observed. First, the metastable ɓ phase, usually called austenite, transforms into the 18R martensitic phase. This transformation can be reversed, with relatively small hysteresis. However, if the sample is further strained, the 18R phase could transform into the 6R martensite, depending on the orientation of the tensile axis. The 6R martensite has an FCT type structure [23]. This phase transition shows stress hysteresis of about 150 MPa [24, 25], whereas the deformation associated to a complete 18Rï 6R transformation is about 10% for a completely transformed material. A noticeable fact which makes this transition extremely interesting for applications is that, starting from the ɓ phase, a reversible deformation of up to approximately 20% can be obtained if a complete ɓï 18Rï 6R transition is produced. In order to induce the 18Rï 6R transformation, the tensile axis must be within about 22Ŭ from the [1 0 0]ɓ direction, otherwise the 18R phase undergoes brittle fracture without a noticeable yield point; occasionally, 2H martensite might be observed after fracture [26].

An important additional detail of this work is based on the fact that the 18R ź 6R transformation and retransformation stresses (ů) show weak temperature dependence. In [27], several reported values for the variation of the critical resolved shear stress with temperature d /dT are mentioned, ranging from ī 0.12 to ī 0.15 MPa/K. Considering the possible tensile orientations, dů/dT might reach an absolute value (as it is always a negative dependence) of up to 0.42 MPa/K. These values are considerably less than those found in the B2 ź B19ô transformation in NiTi (6.3 MPa/K) and also less than those found in the ɓź 18R transformation in polycrystalline CuAlBe alloys (about 2.2 MPa/K), given above.

The slightly negative dů/dT observed in the 18Rï 6R transformation gives the CuZnAl system unique and completely new functionality compared to conventional SMAs, as 10% pseudoelastic strain can be obtained with a stress plateau that is expected to stay almost constant in a wide range of temperatures. Therefore, the use of the 18R ź 6R transformation in damping devices or other applications integrated into mechanical structures would be more advantageous, as ambient temperature changes would cause variations in structure stiffness and resonant frequencies which are smaller than those obtained with other alloys.

In addition, it should be remarked that the hysteresis associated with the 18R ź 6R transformation in CuZnAl single crystals is greater than the hysteresis observed in polycrystalline CuAlBe and comparable to the asymptotic behavior of NiTi alloys after cycling. Moreover, the 18R ź 6R transformation is able to recover more than 10% strain, which is somewhat greater than the recoverable ɓ ź 18R strain in Cu-based alloys and the B2 ź B19ô strain in Niï Ti alloys.

Previous studies [28] show, nevertheless, that the 6R phase in Cuï Znï Al single crystals suffers plastic deformation while it is being formed. This fact renders the mechanical behavior irreversible, creating difficulties for possible engineering implementations of this transformation. Cuniberti and Romero studied the 18Rï 6R transformation in Cuï Znï Al single crystals with electronic concentration e/a = 1.48 and 1.41 and found, by trace analysis, that the 6R slip systems are {1 1 1}FCT[1 1 0]FCT. These authors also reported a slip system whose plane is parallel to the basal plane of the 6R martensite, with a slip direction parallel to [0 1 0]18R, although the corresponding Schmid factor is very small. The [0 1 0]18R is inherited from the [0 1 0]ƀ after the ƀï 18R transition.

As the 18Rï 6R transformation was associated with 6R plastic deformation, the yield stress of the 6R martensite was assumed to be less than or equal to the 18Rï 6R transformation stress.

Although both ƀ ź 18R and 18R ź 6R martensitic transformations can be easily reverted by removing the load, 6R plastic deformation cannot be reverted. Studies in Cuï Alï Ni shape memory alloys have shown that, without precipitation treatments, it is possible to induce the 6R phase in adequately oriented single crystals, without permanent deformation after removing the load. Particularly, it was reported that it is possible to avoid plastic deformation for Ni contents higher than 4 wt.%, whilst plastic deformation of the 6R structure takes place during the 18Rï 6R transition for lower contents of Ni [29]. However, Cuï Alï Ni alloys are more brittle and difficult to manufacture. As a result, Cuï Znï Al alloys can be better choices for certain engineering applications, providing that 6R plastic deformation is controlled.

In this paper it is analyzed the influence of the cooling medium of shape memory alloys from the CuZnAl system on their microstructure and of the phases as part of primary heat treatment education by implementing quenching solution. In the article it is characterized the microstructure of alloys measured by 2D and 3D SEM and AFM.

2. Experimental setup

There were applied to the cast alloys two heat treatments in order to highlight and analyze the martensite. These heat treatments consist in quenching by solution immersion and recovery. The applied heat treatments were performed in a laboratory oven, Vulcan A130 model by heating the samples at 850° C and 900 seconds and keeping cold air cooling (-10° C) or in water at room temperature (25° C). Chemical analysis of the alloys was performed by mass spectrometry using spark Master Foundry equipment for macro-chemical characterization of the material and EDAX measurements (Bruker, GmbH Quantax) for chemical analysis on micro surfaces. XRD analyzes were performed immediately after heat treatment of the samples that were cold polished in order to remove surface oxides formed during heat treatment. The equipment used was X'PERT PRO MRD. For acquisition it was used X'pert Data Collection and for interpretation X'pert High Score Plus. Parameters used to determinations were the Continuous Scan mode, angle range: 20-120 ď using a step size of 0.0131303, time per step: 61.20, scan speed: 0.05471, number of steps: 7616 and as a copper anode X-ray Tube.

Alloy microstructure was determined by scanning electron microscopy (SEM VegaTescan LMH II) on cold mechanically polished samples and chemically attacked with ClFe3 solution. A secondary electron detector (SE) was used to determine the material microstructure to characterize the martensite variants characteristic to the state obtained by solution immersion Cu-based alloys. The 3D analysis, using scanning electron microscopy, was performed using the software VegaTescan / Image operations/3-D view using a 45°, rotation angle and 50° elevation at the Z-scale at 10%. To compare the results obtained with SEM by analyzing 3D at the micron-scale (10 m) martensite variants were characterized also by atomic force microscopy (AFM) using EasyScan II equipment.

3. Results and discussions

Two shape memory alloys of CuZnAl were obtained through classical melting method keeping the mass and atomic percentages of chemical elements in proper ranges to exhibit shape memory effect. These alloys were poured in lamella shape and heat treated to highlight the martensitic state of the materials. The materials were heated to 850 °C maintained for 900 seconds and cooled in cold air and water at room temperature. These alloys were named as alloy 1 and alloy 2. By chemical considerations point of view the new obtained materials were analyzed through mass spectroscopy and EDAX (X-ray energy dispersive analyze) and the alloy compositions are shown in table 1.

The materials present a good chemical homogeneity at macro and micro scale with reduce differences between the results.

For samples cooled from the ƀ phase region of high temperature of copper-based alloys with shape memory, it can be observed a martensitic transformation L21 Ÿ M18R type. Using the XRD technique, the network parameters of 9 or 18R orthorhombic structure type and the changes that occur due the cooling medium variation can be observed and analyzed.

Alloy no.1 shows predominant ƀ phase with empirical formula Cu0.61Zn0.39 and lower rates of Al3Cu2 and CuZn5 phases.

The shape memory effect observed in many alloys systems represents a thermoelastic martensitic transformation direct result [8-10]. This transformation is crystallographic reversible and represents the base of the shape recovery mechanism. For a better understanding of shape memory alloys based on CuZnAl that are presenting a thermoelastic martensitic transformation, the studies based on X ï ray analysis are very important. For noble shape memory alloys the phase matrix at high temperature

is a disorder - bcc (A2) type. The bcc phase presents on cooling two ordering transitions during cooling. The first cooling transition represents an ordering reaction of the closest phases (near neighbor - nn) that leads to a B2 type matrix (CsCl type) called ɓ2. A further cooling induces another ordering of the following phases from the crystalline structure and it will become the DO3 (Fe3Al type) also called ɓ1 or L21.

Atoms sizes have an important effect on the formation of ordered structures [11]. However, some researchers [9, 12] affirm the fact that DO3 perfect matrices will never be found in CuZnAl alloys and the resulting structure by the above described mechanism could be a L21 matrix. A2 disordered phase transformations in the basic phase B2 occurs during quenching in water [8] because the transition from B2 to L2 phase can be suppressed by quenching in water after a preliminary homogenization treatment.

Table 1 Chemical compositions of experimented shape memory alloys.

Alloy number	Mass percentages %			Atomic percentages %		
	Cu	Zn	Al	Cu	Zn	Al
Alloy 1 (spectr.)	75.5	19.7	4.8	71.2	18.05	10.67
Alloy 1 (EDAX)	75.5	19.6	4.86	71.2	17.96	10.8
Alloy 2 (spectr.)	70.4	24	5.6	65.9	21.82	12.34
Alloy 2 (EDAX)	70.8	24.82	5.41	65.8	22.40	11.85

Fig. 1 presents the alloys diffractograms 1 in a) and 2 in b) for both air cooling and in cold water.

The lines observed in diffractograms were identified as M18R martensite superlattice reflections and attributed on the orthorhombic system. Plane spacing of diffraction planes in CuZnAl alloys shown in Fig. 1 processed with two various conditions can be observed.

Bigger splitting and spacing distances are observed in cold air cooling experiments so the degree of ordering in the 18R martensite type is smaller than the degree from alloy quenched in water in both cases. One of the most important conditions for shape memory effect exhibition in SMA is structural ordering. Usually the structure of CuZnAl shape memory alloys is inhibited from the parent phase existing prior to the transformation. If the atoms are randomly distributed in the basal plane the ratio a/b of the lattice parameters should be equal to sqrt3/2 for 18R martensites. But the basal plane consist of atoms of different dimensions and during the parent phase ordering the a/b ratio is less than 0.866 for 18R martensites. In our case, the lattice parameters presented in table 2, the ratio is 0.861 and this deviation from ideal values of a/b results in splitting of certain diffraction lines in the orthorhombic martensite phase.

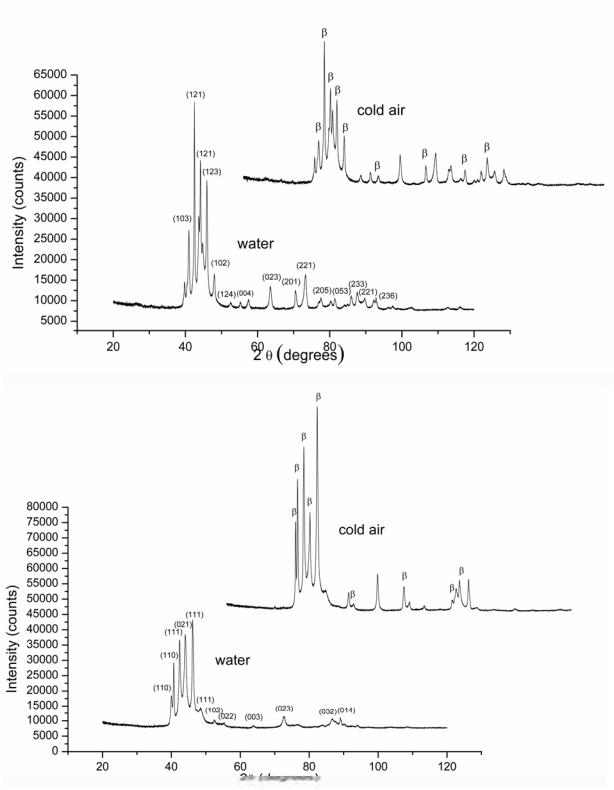

Fig. 1. X-ray shape memory alloys diffractograms of the samples of alloys one in water and cold air and second in similar conditions a) alloy 1 and b) alloy 2

The structure of ɓ martensite in copper based materials is based on one of the {110} basal planes in which the atoms are shifted or adjusted slightly in accordance with the tetragonal distortion of martensite [12-14].

Table 2 Lattice parameters of β phase of the specimens.

Alloy	Lattice parameters for ɓ phase				Cell volume
	a (Å)	b (Å)	c (Å)	ɓ	
Alloy 1/cold air	4.275	4.964	32.678	90°	51.11
Alloy 1/water	4.272	4.962	32.674	90°	50.97
Alloy 2/cold air	4.273	4.963	32.675	90°	51.01
Alloy 2/water	4.271	4.961	32.672	90°	50.91

For alloys 1and 2, especially for the second one, in cold air cooled sample cases residual austenite peaks can be also observed on the XRD diffractograms.

The shape memory alloy 1 present a martensitic structure after both cooling methods. The variants dimensions, orientation and homogeneity are analyzed using scanning electrons microscope and atomic force microscope. Micro-structural considerations of shape memory alloy 1 are presented in figure 2 for 500x and 5000x amplifications of structure. 3D investigations are also made using scanning electrons microscope and atomic force microscope for complete martensitic variants characterization.

Macroscopic the alloy 1 structure present in both cases (cooled in cold air, a) and in water at room temperature, d)) a homogeneous structure with well defined grains. The martensite variants are especially as arrowhead with the same orientation in cold air cooled sample case, in diamond shapes and also plates with different orientations. In cold air cooled sample the grains dimensions vary between 110 and 145 μm length, around 50 areas of the same sample were investigated and measured and an average of 25 grains for cold air cooled sample and 15 grains for water quenched on a 0.25 mm^2 surface, comparing with the water cooled sample that present reduced areas with small grains, around 50 μm in length, and areas with long martensitic variants with lengths bigger than 200 μm being a favorable structure for shape memory effect.

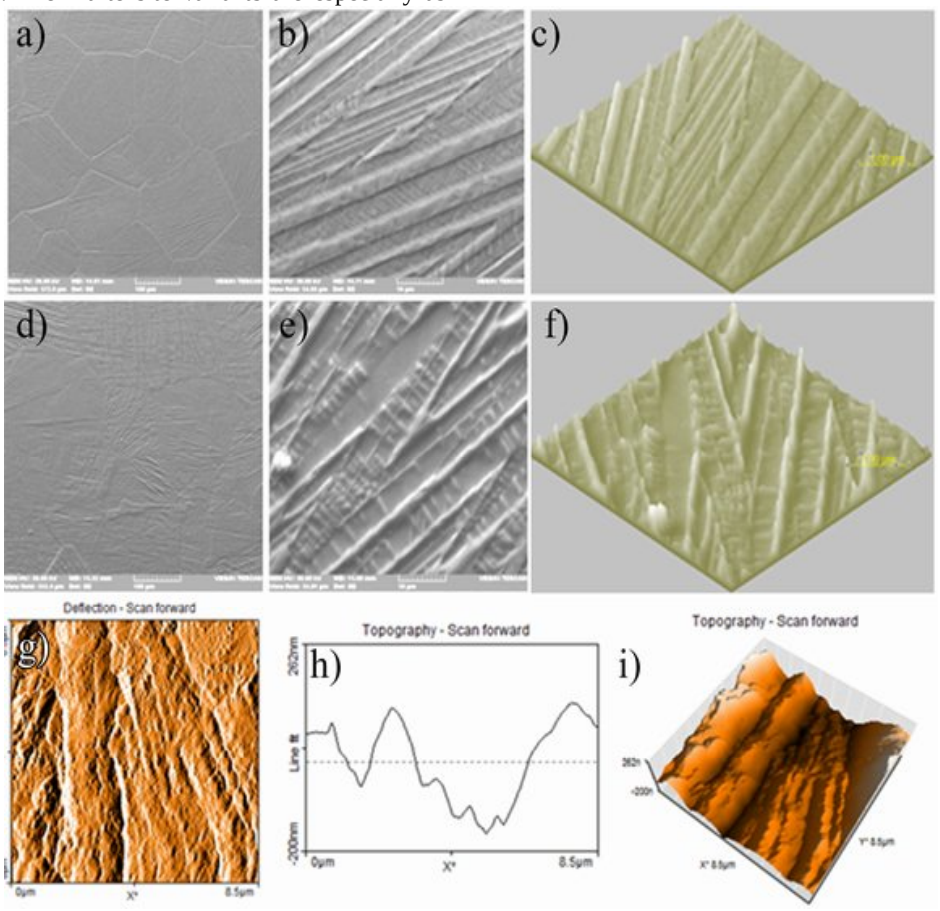

Fig. 2. SEM and AFM investigations of shape memory alloy 1 structure after the quenching heat treatment with cooling in cold air, a), b) and c) and water in d), e) and f), AFM results are presented in g), h) and i).

At micro-scale primer and secondary variants can be observed in both cases with 2-5 μm width and an average of 2.2 μm in air cold cooled sample and 1.8 μm for sample quenched in water (the average was obtained after 100 measurements of martensite variants). The secondary variants are about 200 nm in air cooled case and 500 nm for sample treated in water. The angle orientation between martensite variants is usually at 45 ° and the plates have an approximate height of 400 nm for primary plates and 200 nm for secondary variants determined from 3D acquisitions with SEM and AFM. All these results are obtained on samples mechanically prepared and chemically attacked fact that influence the real values in height of the martensitic variants but as a comparative study are important to establish the differences between these two samples.

The results with SEM and AFM of second alloy analyze are presented in figure 3 for both cooling conditions. In the first case, cold air cooled, macro-structural aspects presents martensitic grains with lengths between 50 and 150 μm, around 50 areas of the same sample were investigated and measured and an average of

28 grains for cold air cooled sample and 2 grains for water quenched on a 0.25 mm^2 surface, comparing with the water cooled sample that present big areas with martensitic variants, around 500 µm in length, favourable for shape memory effect.

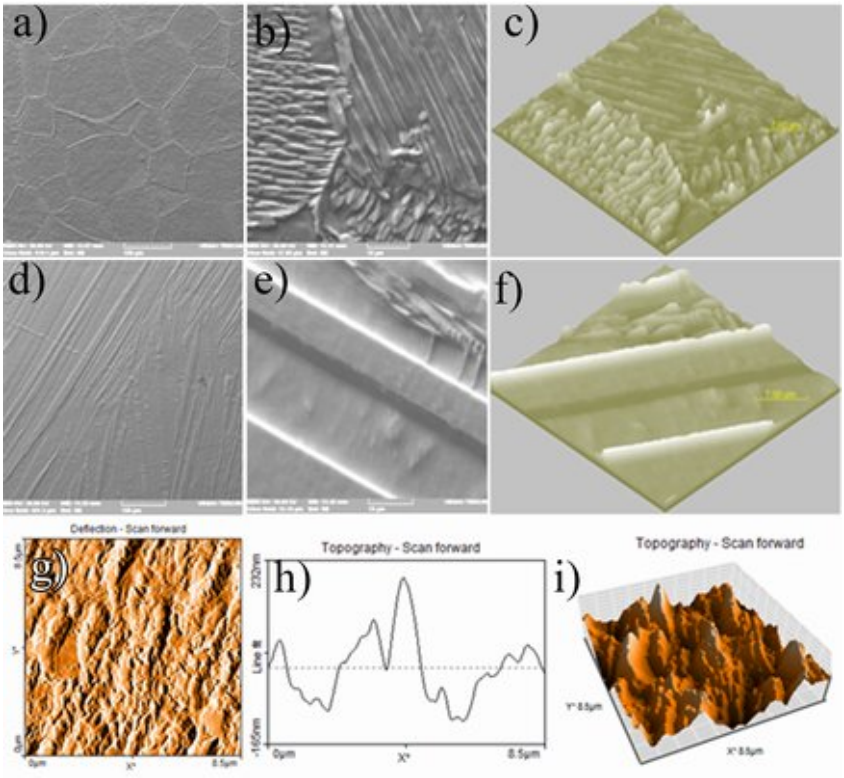

Fig. 3 SEM and AFM investigations of shape memory alloy 2 structure after the quenching heat treatment with cooling in cold air, a), b) and c) and water in d), e) and f) ,AFM results are presented in g), h) and i).

In the first case among the martensite variants the microstructure presents the residual austenite phase participation, figure 3 b), with a reduced percentage (less than 10%) between the martensitic grains.

At micro-scale primer, in both cases, and secondary, only in water cooled case, variants can be observed with a 0.5-0.75 µm width and an average of 0.68 µm in air cold cooled sample and 2-3 µm width and an average of 2.8 µm for sample quenched in water (the average was obtained after 100 measurements of martensite variants). The secondary variants are about 100 nm for sample treated in water. The angle orientation between martensite variants is usually at 45° and the plates have an approximate height of 400 nm for primary plates and 100 nm for secondary variants determined from 3D acquisitions with SEM and AFM. The shape memory alloy surface relief is obtained after mechanical preparation of the sample and chemical attack fact that amplify the martensite variants dimensions but keep the morphology intact.

The topographies present also differences of height between the primary and secondary martensitic variants. A better highlighting between primary and secondary variants is observed in alloy 1 case from AFM 3D result comparing with the second alloy, figure 2 i) and 3 i).

Shape memory effect, one of the most used properties of SMAs, is closely related to the microstructure transformation with temperature variation. The reverse of the microstructure from disorder austenite phase to initial martensite ordered state in the same order is one of the key controls of smart materials.

Scanning electrons microscope and atomic force microscope can establish the microstructure return in initial shape and using proper thermo-mechanical treatments an almost perfect shape memory alloy can be obtained. This idea can be realized using at the beginning a single crystal material or a simpler system like two elements NiTi shape memory alloy.

A proper solution to control the microstructure and directly the shape memory effect of the smart materials is to obtain martensite variants at nano-scale with a trained behavior and easier control. This way the memory effect will be amplified, better controlled and with a superior action rate. A solution to transform the martensite micro-variants in nano-variants is through severe deformation that can be easily applied to copper based shape memory alloy.

4. Conclusions

Two shape memory copper based alloys were obtained through classical method. Both alloys were analyzed by primer heat treatment apply for two different

cooling environments. The transformation from ϭ phase to martensitic phase is L21 for both cooling conditions of the alloys studied in this paper. It has been found that M18R orthorhombic martensitic structure transformed from ϭ phase is ordered in all cases. Cooling in cold air the second shape memory sample presents a percentage of residual austenite phase.

Micro-structural investigations characterize, paying respect for the chemical attack influence on microstructure dimensions, the martensite aspects at macro and microscopic scale.

The conditions applied for 3D analysis with scanning electron microscopy satisfy the values recorded by atomic force microscopy thus obtaining a new method for analyzing surface condition. Advantages of 3D analysis using the SEM are given by the investigated surface sizes (at the AFM equipment these are limited by the sensor model to 10x10 or 100x100 εm^2), in many cases the material surface roughness, speed of obtaining the results and the possibility of pieces and samples analysis with a complex geometry without damaging the structure.

Acknowledgement

This paper was realized with the support of POSDRU CUANTUMDOC ñDOCTORAL STUDIES FOR EUROPEAN PERFORMANCES IN RESEARCH AND INOVATIONò ID79407 project funded by the European Social Found and Romanian Government.

Partial of this work was supported by a grant of the Romanian National Authority for Scientific Research, CNCS ï UEFISCDI, project number PN-II-RU-PD-2011-3-0186.

References

[1] L. G. Bujoreanu, N. M. Lohan, B. Pricop, N. Cimpoeкu, J. of Mater. Eng. and Perform., **20**, 468 (2011).
[2] G. S. Yang, J. K. Lee, W. Y. Jang, Trans. Nonferrous Met. Soc. China **19**, 979 (2009).
[3] S. Montecinos, S.N. Simison, Appl. Surf. Sci. **257**, 7732 (2011).
[4] N. Cimpoeкu, S. Stanciu, M. Meyer, I. IoniŞ, R. Cimpoeкu Hanu, J. Optoelectron. Adv. Mater. **12,** 386 (2010).
[5] O.Adigüzel, Mater. Res. Bull. **30**, 755 (1995).
[6] D.W. Roh, E.S. Lee, Y.G. Kim, Metall. Trans. A **23A**, 2753 (1992).
[7] G,Vitel., A. L. Paraschiv, M. G. Suru, N. Cimpoesu L. ï G. Bujoreanu, Optoelectron. Adv. Mater. Rapid Commun., **5**, 858 (2011).
[8] L.-G Bujoreanu., N. M. Lohan; B. Pricop; N. Cimpoeкu, Mater. Sci. Techn., DOI: http://dx.doi.org/10.1179/ 1743 284711Y.0000000099, 2012.
[9] M. Benke, V. Mertinger, L. Daroczi, J. Mater. Eng. Perform. **18**, 496 (2009).
[10] M. Eskil, N. Kayali, Mater. Lett. **60**, 630 (2006).
[11] N. Cimpoesu, M. Axinte, R. Cimpoesu Hanu, C. Nejneru, D. C. Achitei, S. Stanciu, J. Optoelectron. Adv. Mater. **12**, 1772 (2010) .
[12] S. N. Balo, N. Sel, Thermochim. Acta **536,** 1 (2012).
[13] G. Vitel, A. L. Paraschiv, M. G. Suru, N. Cimpoeкu, L.-G. Bujoreanu, Optoelectron. Adv. Mater. Rapid Commun. **6**, 339 (2012).
[14] C. Tatar, Thermochim. Acta **437**, 121 (2005).
[15] T. Saburi, in: K. Otsuka, C.M. Wayman (Eds.), Shape Memory Materials, Cambridge University Press, Cambridge, UK, 1998, pp. 49ï 96.
[16] J. Olbricht, A. Yawny, A.M. Condó, F.C. Lovey, G. Eggeler, Mater. Sci. Eng. A **481–482**, 142 (2008).
[17] J.F. Beltran, C. Cruz, R. Herrera, O. Moroni, Eng. Struct. **33**, 2910 (2011).
[18] S. Montecinos, A. Cuniberti, J. Alloys Compd. **457**, 332 (2008).
[19] S. Montecinos, A. Cuniberti, A. Sepúlveda, Mater. Charact. **59**, 117 (2008).
[20] S.H. Chang, Mater. Chem. Phys. **125**, 358 (2011).
[21] M. Barrado, G.A. López, M.L. Nó, J. San Juan, Mater. Sci. Eng. A **521–522**, 363 (2009).
[22] U.S. Mallik, V. Sampath, Mater. Sci. Eng. A **478**, 48 (2008).
[23] A. Baruj, T. Kikuchi, S. Kajiwara, N. Shinya, Mater. Trans. **43**, 585 (2002).
[24] J.L. Pelegrina, M. Ahlers, Acta Metall. Mater. **40**, 3205 (1992).
[25] M. Ahlers, J.L. Pelegrina, Acta Metall. Mater. **40**, 3213 (1992).
[26] P. Wollants, J.R. Ross, L. Delaey, Prog. Mater. Sci. **37**, 227 (1993).
[27] F. Saule, M. Ahlers, Acta Metall. Mater. **43**, 2373 (1995).
[28] M. Sade, R. Rapacioli, F.C. Lovey, M. Ahlers, J. Phys. **C4–43**, 647 (1982).
[29] L. Delaey, J. Janssen, J. Van Humbeeck, J. Luyten, A. Deruyttere, Proc. ICOMAT 1979, Cambridge, MA, 1979, 645ï 648.

*Corresponding author: nicanornick@yahoo.com0